Research Papers in Physics and Astronomy

Gregory Snow Publications

University of Nebraska - Lincoln *Year* 2001

Search for dilepton signatures from minimal low-energy supergravity in $pp?$ collisions at $?s = 1.8$ TeV

B. Abbott* Gregory Snow†

D0 Collaboration‡

*New York University, New York, New York 10003

†gsnow@unlhep.unl.edu

‡

PHYSICAL REVIEW D, VOLUME 63, 091102(R)

Search for dilepton signatures from minimal low-energy supergravity in $p\bar{p}$ collisions at $\sqrt{s}=1.8$ TeV

B. Abbott,[50] M. Abolins,[47] V. Abramov,[23] B. S. Acharya,[15] D. L. Adams,[57] M. Adams,[34] G. A. Alves,[2] N. Amos,[46] E. W. Anderson,[39] M. M. Baarmand,[52] V. V. Babintsev,[23] L. Babukhadia,[52] A. Baden,[43] B. Baldin,[33] P. W. Balm,[18] S. Banerjee,[15] J. Bantly,[56] E. Barberis,[26] P. Baringer,[40] J. F. Bartlett,[33] U. Bassler,[11] A. Bean,[40] M. Begel,[51] A. Belyaev,[22] S. B. Beri,[13] G. Bernardi,[11] I. Bertram,[24] A. Besson,[9] V. A. Bezzubov,[23] P. C. Bhat,[33] V. Bhatnagar,[13] M. Bhattacharjee,[52] G. Blazey,[35] S. Blessing,[31] A. Boehnlein,[33] N. I. Bojko,[23] F. Borcherding,[33] A. Brandt,[57] R. Breedon,[27] G. Briskin,[56] R. Brock,[47] G. Brooijmans,[33] A. Bross,[33] D. Buchholz,[36] M. Buehler,[34] V. Buescher,[51] V. S. Burtovoi,[23] J. M. Butler,[44] F. Canelli,[51] W. Carvalho,[3] D. Casey,[47] Z. Casilum,[52] H. Castilla-Valdez,[17] D. Chakraborty,[52] K. M. Chan,[51] S. V. Chekulaev,[23] D. K. Cho,[51] S. Choi,[30] S. Chopra,[53] B. C. Choudhary,[30] J. H. Christenson,[33] M. Chung,[34] D. Claes,[48] A. R. Clark,[26] J. Cochran,[30] L. Coney,[38] B. Connolly,[31] W. E. Cooper,[33] D. Coppage,[40] M. A. C. Cummings,[35] D. Cutts,[56] O. I. Dahl,[26] G. A. Davis,[51] K. Davis,[25] K. De,[57] K. Del Signore,[46] M. Demarteau,[33] R. Demina,[41] P. Demine,[9] D. Denisov,[33] S. P. Denisov,[23] S. Desai,[52] H. T. Diehl,[33] M. Diesburg,[33] G. Di Loreto,[47] S. Doulas,[45] P. Draper,[57] Y. Ducros,[12] L. V. Dudko,[22] S. Duensing,[19] S. R. Dugad,[15] A. Dyshkant,[23] D. Edmunds,[47] J. Ellison,[30] V. D. Elvira,[33] R. Engelmann,[52] S. Eno,[43] G. Eppley,[59] P. Ermolov,[22] O. V. Eroshin,[23] J. Estrada,[51] H. Evans,[49] V. N. Evdokimov,[23] T. Fahland,[29] S. Feher,[33] D. Fein,[25] T. Ferbel,[51] H. E. Fisk,[33] Y. Fisyak,[53] E. Flattum,[33] F. Fleuret,[26] M. Fortner,[35] K. C. Frame,[47] S. Fuess,[33] E. Gallas,[33] A. N. Galyaev,[23] P. Gartung,[30] V. Gavrilov,[21] R. J. Genik II,[24] K. Genser,[33] C. E. Gerber,[34] Y. Gershtein,[56] B. Gibbard,[53] R. Gilmartin,[31] G. Ginther,[51] B. Gómez,[5] G. Gómez,[43] P. I. Goncharov,[23] J. L. González Solís,[17] H. Gordon,[53] L. T. Goss,[58] K. Gounder,[30] A. Goussiou,[52] N. Graf,[53] G. Graham,[43] P. D. Grannis,[52] J. A. Green,[39] H. Greenlee,[33] S. Grinstein,[1] P. Grudberg,[26] S. Grünendahl,[33] A. Gupta,[15] S. N. Gurzhiev,[23] G. Gutierrez,[33] P. Gutierrez,[55] N. J. Hadley,[43] H. Haggerty,[33] S. Hagopian,[31] V. Hagopian,[31] K. S. Hahn,[51] R. E. Hall,[28] P. Hanlet,[45] S. Hansen,[33] J. M. Hauptman,[39] C. Hays,[49] C. Hebert,[40] D. Hedin,[35] A. P. Heinson,[30] U. Heintz,[44] T. Heuring,[31] R. Hirosky,[34] J. D. Hobbs,[52] B. Hoeneisen,[8] J. S. Hoftun,[56] S. Hou,[46] Y. Huang,[46] A. S. Ito,[33] S. A. Jerger,[47] R. Jesik,[37] K. Johns,[25] M. Johnson,[33] A. Jonckheere,[33] M. Jones,[32] H. Jöstlein,[33] A. Juste,[33] S. Kahn,[53] E. Kajfasz,[10] D. Karmanov,[22] D. Karmgard,[38] R. Kehoe,[38] S. K. Kim,[16] B. Klima,[33] C. Klopfenstein,[27] B. Knuteson,[26] W. Ko,[27] J. M. Kohli,[13] A. V. Kostritskiy,[23] J. Kotcher,[53] A. V. Kotwal,[49] A. V. Kozelov,[23] E. A. Kozlovsky,[23] J. Krane,[39] M. R. Krishnaswamy,[15] S. Krzywdzinski,[33] M. Kubantsev,[41] S. Kuleshov,[21] Y. Kulik,[52] S. Kunori,[43] V. E. Kuznetsov,[30] G. Landsberg,[56] A. Leflat,[22] F. Lehner,[33] J. Li,[57] Q. Z. Li,[33] J. G. R. Lima,[3] D. Lincoln,[33] S. L. Linn,[31] J. Linnemann,[47] R. Lipton,[33] A. Lucotte,[52] L. Lueking,[33] C. Lundstedt,[48] A. K. A. Maciel,[35] R. J. Madaras,[26] V. Manankov,[22] S. Mani,[27] H. S. Mao,[4] T. Marshall,[37] M. I. Martin,[33] R. D. Martin,[34] K. M. Mauritz,[39] B. May,[36] A. A. Mayorov,[37] R. McCarthy,[52] J. McDonald,[31] T. McMahon,[54] H. L. Melanson,[33] X. C. Meng,[4] M. Merkin,[22] K. W. Merritt,[33] C. Miao,[56] H. Miettinen,[59] D. Mihalcea,[55] A. Mincer,[50] C. S. Mishra,[33] N. Mokhov,[33] N. K. Mondal,[15] H. E. Montgomery,[33] M. Mostafa,[1] H. da Motta,[2] E. Nagy,[10] F. Nang,[25] M. Narain,[44] V. S. Narasimham,[15] H. A. Neal,[46] J. P. Negret,[5] S. Negroni,[10] D. Norman,[58] L. Oesch,[46] V. Oguri,[3] B. Olivier,[11] N. Oshima,[33] P. Padley,[59] L. J. Pan,[36] A. Para,[33] N. Parashar,[45] R. Partridge,[56] N. Parua,[9] M. Paterno,[51] A. Patwa,[52] B. Pawlik,[20] J. Perkins,[57] M. Peters,[32] O. Peters,[18] R. Piegaia,[1] H. Piekarz,[31] B. G. Pope,[47] E. Popkov,[38] H. B. Prosper,[31] S. Protopopescu,[53] J. Qian,[46] P. Z. Quintas,[33] R. Raja,[33] S. Rajagopalan,[53] E. Ramberg,[33] P. Rapidis,[33] N. W. Reay,[41] S. Reucroft,[45] J. Rha,[30] M. Rijssenbeek,[52] T. Rockwell,[47] M. Roco,[33] P. Rubinov,[33] R. Ruchti,[38] J. Rutherfoord,[25] A. Santoro,[2] L. Sawyer,[42] R. D. Schamberger,[52] H. Schellman,[36] A. Schwartzman,[1] J. Sculli,[50] N. Sen,[59] E. Shabalina,[22] H. C. Shankar,[15] R. K. Shivpuri,[14] D. Shpakov,[52] M. Shupe,[25] R. A. Sidwell,[41] V. Simak,[7] H. Singh,[30] J. B. Singh,[13] V. Sirotenko,[33] P. Slattery,[51] E. Smith,[55] R. P. Smith,[33] R. Snihur,[36] G. R. Snow,[48] J. Snow,[54] S. Snyder,[53] J. Solomon,[34] V. Sorín,[1] M. Sosebee,[57] N. Sotnikova,[22] K. Soustruznik,[6] M. Souza,[2] N. R. Stanton,[41] G. Steinbrück,[49] R. W. Stephens,[57] M. L. Stevenson,[26] F. Stichelbaut,[53] D. Stoker,[29] V. Stolin,[21] D. A. Stoyanova,[23] M. Strauss,[55] K. Streets,[50] M. Strovink,[26] L. Stutte,[33] A. Sznajder,[3] W. Taylor,[52] S. Tentindo-Repond,[31] J. Thompson,[43] D. Toback,[43] T. G. Trippe,[26] A. S. Turcot,[53] P. M. Tuts,[49] P. van Gemmeren,[33] V. Vaniev,[23] R. Van Kooten,[37] N. Varelas,[34] A. A. Volkov,[23] A. P. Vorobiev,[23] H. D. Wahl,[31] H. Wang,[36] Z.-M. Wang,[52] J. Warchol,[38] G. Watts,[60] M. Wayne,[38] H. Weerts,[47] A. White,[57] J. T. White,[58] D. Whiteson,[26] J. A. Wightman,[39] D. A. Wijngaarden,[19] S. Willis,[35] S. J. Wimpenny,[30] J. V. D. Wirjawan,[58] J. Womersley,[33] D. R. Wood,[45] R. Yamada,[33] P. Yamin,[53] T. Yasuda,[33] K. Yip,[33] S. Youssef,[31] J. Yu,[33] Z. Yu,[36] M. Zanabria,[5] H. Zheng,[38] Z. Zhou,[39] Z. H. Zhu,[51] M. Zielinski,[51] D. Zieminska,[37] A. Zieminski,[37] V. Zutshi,[51] E. G. Zverev,[22] and A. Zylberstejn[12]

(DØ Collaboration)

[1]*Universidad de Buenos Aires, Buenos Aires, Argentina*
[2]*LAFEX, Centro Brasileiro de Pesquisas Físicas, Rio de Janeiro, Brazil*
[3]*Universidade do Estado do Rio de Janeiro, Rio de Janeiro, Brazil*
[4]*Institute of High Energy Physics, Beijing, People's Republic of China*
[5]*Universidad de los Andes, Bogotá, Colombia*
[6]*Charles University, Prague, Czech Republic*
[7]*Institute of Physics, Academy of Sciences, Prague, Czech Republic*

[8]*Universidad San Francisco de Quito, Quito, Ecuador*
[9]*Institut des Sciences Nucléaires, IN2P3-CNRS, Universite de Grenoble 1, Grenoble, France*
[10]*CPPM, IN2P3-CNRS, Université de la Méditerranée, Marseille, France*
[11]*LPNHE, Universités Paris VI and VII, IN2P3-CNRS, Paris, France*
[12]*DAPNIA/Service de Physique des Particules, CEA, Saclay, France*
[13]*Panjab University, Chandigarh, India*
[14]*Delhi University, Delhi, India*
[15]*Tata Institute of Fundamental Research, Mumbai, India*
[16]*Seoul National University, Seoul, Korea*
[17]*CINVESTAV, Mexico City, Mexico*
[18]*FOM-Institute NIKHEF and University of Amsterdam/NIKHEF, Amsterdam, The Netherlands*
[19]*University of Nijmegen/NIKHEF, Nijmegen, The Netherlands*
[20]*Institute of Nuclear Physics, Kraków, Poland*
[21]*Institute for Theoretical and Experimental Physics, Moscow, Russia*
[22]*Moscow State University, Moscow, Russia*
[23]*Institute for High Energy Physics, Protvino, Russia*
[24]*Lancaster University, Lancaster, United Kingdom*
[25]*University of Arizona, Tucson, Arizona 85721*
[26]*Lawrence Berkeley National Laboratory and University of California, Berkeley, California 94720*
[27]*University of California, Davis, California 95616*
[28]*California State University, Fresno, California 93740*
[29]*University of California, Irvine, California 92697*
[30]*University of California, Riverside, California 92521*
[31]*Florida State University, Tallahassee, Florida 32306*
[32]*University of Hawaii, Honolulu, Hawaii 96822*
[33]*Fermi National Accelerator Laboratory, Batavia, Illinois 60510*
[34]*University of Illinois at Chicago, Chicago, Illinois 60607*
[35]*Northern Illinois University, DeKalb, Illinois 60115*
[36]*Northwestern University, Evanston, Illinois 60208*
[37]*Indiana University, Bloomington, Indiana 47405*
[38]*University of Notre Dame, Notre Dame, Indiana 46556*
[39]*Iowa State University, Ames, Iowa 50011*
[40]*University of Kansas, Lawrence, Kansas 66045*
[41]*Kansas State University, Manhattan, Kansas 66506*
[42]*Louisiana Tech University, Ruston, Louisiana 71272*
[43]*University of Maryland, College Park, Maryland 20742*
[44]*Boston University, Boston, Massachusetts 02215*
[45]*Northeastern University, Boston, Massachusetts 02115*
[46]*University of Michigan, Ann Arbor, Michigan 48109*
[47]*Michigan State University, East Lansing, Michigan 48824*
[48]*University of Nebraska, Lincoln, Nebraska 68588*
[49]*Columbia University, New York, New York 10027*
[50]*New York University, New York, New York 10003*
[51]*University of Rochester, Rochester, New York 14627*
[52]*State University of New York, Stony Brook, New York 11794*
[53]*Brookhaven National Laboratory, Upton, New York 11973*
[54]*Langston University, Langston, Oklahoma 73050*
[55]*University of Oklahoma, Norman, Oklahoma 73019*
[56]*Brown University, Providence, Rhode Island 02912*
[57]*University of Texas, Arlington, Texas 76019*
[58]*Texas A&M University, College Station, Texas 77843*
[59]*Rice University, Houston, Texas 77005*
[60]*University of Washington, Seattle, Washington 98195*

(Received 9 February 2000; published 10 April 2001)

We report on a search for supersymmetry using the DØ detector. The 1994–1996 data sample of $\sqrt{s}=1.8$ TeV $p\bar{p}$ collisions was analyzed for events containing two leptons (e or μ), two or more jets, and missing transverse energy. Assuming the minimal supergravity model, with $A_0=0$ and $\mu<0$, various thresholds were employed to optimize the search. No events were found beyond expectation from the background. We set a

lower limit at the 95% C.L. of 255 GeV/c^2 for equal mass squarks and gluinos for $\tan\beta=2$, and present exclusion contours in the $(m_0, m_{1/2})$ plane for $\tan\beta=2$–6.

DOI: 10.1103/PhysRevD.63.091102 PACS number(s): 12.60.Jv, 04.65.+e, 13.85.Rm, 14.80.Ly

Supersymmetric extensions of the standard model (SM) have been the subject of intense theoretical and experimental investigation in recent years. The simplest, the minimal supersymmetric standard model (MSSM), incorporates supersymmetry (SUSY) [1], a fundamental space-time symmetry relating fermions to bosons. SUSY requires the existence of a partner (a sparticle) for every SM particle, and at least one additional Higgs doublet. The added assumption of conservation of R-parity, a multiplicative quantum number ($+1$ for SM particles and -1 for their SUSY counterparts), implies the pair production of sparticles in high energy collisions. The sparticles can decay directly, or via lighter sparticles, into final states containing SM particles and stable lightest supersymmetric particles (LSPs). LSPs are weakly interacting objects [2] that escape detection and produce a large apparent imbalance in transverse energy ($\not\!\!E_T$) in the event. This is a characteristic signature for SUSY processes.

In this Rapid Communication we describe a search for production of squarks ($\tilde{q}$), gluinos ($\tilde{g}$), charginos ($\tilde{\chi}^{\pm}_{1-2}$), and/or neutralinos ($\tilde{\chi}^0_{1-4}$). Cascade decays of these sparticles can have significant leptonic branching fractions. For example, $\tilde{g}$ cascades can terminate with the decay $\tilde{\chi}^0_2 \rightarrow l\bar{l}\tilde{\chi}^0_1$ 25% of the time [3]. We consider final states containing two isolated leptons (e or μ), two or more jets (or three or more jets), and $\not\!\!E_T$ [3], thus complementing searches that consider only jets and $\not\!\!E_T$ [4]. Such dilepton final states provide much cleaner signals with greatly reduced instrumental backgrounds from misidentified primary interaction vertices and QCD multijet production.

Because of the large number of free parameters in the generic MSSM, we have chosen to compare our data with a class of minimal low-energy supergravity (mSUGRA) models [5,6] that are more tightly constrained. Within these models, all forces are unified at energy below the Planck scale (10^{19} GeV), near 10^{16} GeV, where gravity couples degenerate particles and sparticles. This particle-sparticle symmetry is broken below the unification scale.

The models are parametrized in terms of only five free parameters: a common SUSY-breaking mass (m_0) for all scalars (e.g. the $\tilde{q}$ mass), a common mass ($m_{1/2}$) for all gauginos (e.g. the $\tilde{g}$ mass), a common value for all trilinear couplings (A_0), the ratio of the vacuum expectation values of the two Higgs fields ($\tan\beta$), and the sign of μ, where μ is the Higgsino mass parameter. The masses and couplings at the weak scale are obtained from the unification scale parameters upon solving the renormalization group equations. This running down to the weak scale can increase or decrease sparticle masses from their common unification scale values, depending upon the choice of free parameters. One of the attractions of these models is that they lead naturally to electroweak symmetry breaking, without additional assumptions. In this analysis, we take $A_0=0$ because to first order the trilinear couplings are expected to have no effect on production and decay mechanisms. In addition, we assume $\mu<0$ because positive values of μ lead to smaller splittings in gaugino masses and produce leptons in cascade decays that are below detection thresholds at DØ.

The DØ detector [7] consists of a liquid-argon calorimeter surrounding central tracking chambers, all enclosed within an iron toroidal muon spectrometer. Structurally, the calorimeter is segmented into a central calorimeter (CC) and two end calorimeters (EC). Within the central tracking chambers, a transition radiation detector (TRD) aids in electron identification in the CC.

The data were collected during the 1994–1996 Fermilab Tevatron collider run. We triggered on an electron, one jet, and $\not\!\!E_T$, for the ee and $e\mu$ signatures, and on a muon and a jet for the $\mu\mu$ signatures. The integrated luminosity was 108 ± 6 pb^{-1} for ee and $e\mu$ signatures, and 103 ± 5 pb^{-1} for $\mu\mu$ signatures. The original data sample of several 10^6 events was reduced by requiring that events have two leptons satisfying loose identification criteria, two jets with $E_T>15$ GeV, and $\not\!\!E_T>14$ GeV. This sample of 24 233 predominantly multijet events was used in the subsequent analysis.

Jets were reconstructed from the energy deposition in the calorimeter in cones of radius $\mathcal{R}=\sqrt{(\Delta\eta)^2+(\Delta\phi)^2}=0.5$, where ϕ is the azimuthal angle with respect to the beam axis and η is the pseudorapidity. Additional details concerning reconstruction and energy calibration can be found in Refs. [7–9]. Jets were required to be in the region $|\eta|<2.5$.

We selected electrons in the CC ($|\eta|<1.1$) and in the EC ($1.5<|\eta|<2.5$) using, respectively, a 5-variable and a 4-variable likelihood function based on the fraction of energy deposited in the electromagnetic (EM) portion of the calorimeter, a shower-shape variable, track ionization (dE/dx) in the central detector, the quality of the match between the reconstructed track and the center of gravity of the calorimeter cluster ($\sigma_{\rm TRK}$), and a variable based on the energy deposited in the TRD (not used for the EC). The identification efficiency for electrons was determined using a sample of $Z\rightarrow ee$ events, and depends on jet multiplicity (high track-multiplicity degrades the resolution of $\sigma_{\rm TRK}$). We defined an electron isolation variable $\mathcal{I}=(E^{0.4}_{\rm tot}-E^{0.2}_{\rm EM})/(E^{0.2}_{\rm EM})$, where $E^{0.2}_{\rm EM}$ is the EM energy in a cone of $\mathcal{R}=0.2$ and $E^{0.4}_{\rm tot}$ is the total calorimeter energy in a cone of $\mathcal{R}=0.4$. We required $\mathcal{I}<0.3$ in this analysis. The identification efficiencies for isolated electrons were typically 78–84 % for CC electrons, and 63–69 % for EC electrons [3].

Muon identification is detailed in Ref. [9]. Muons were required to have $|\eta|<1.7$ and to lie outside of all reconstructed jets defined by $\mathcal{R}=0.5$ cones. To remove poorly measured muon momenta, the direction of the vector $\not\!\!E_T$ was required to be more than 10 degrees in ϕ away from any muon track; this reduced the acceptance by about 10% per muon.

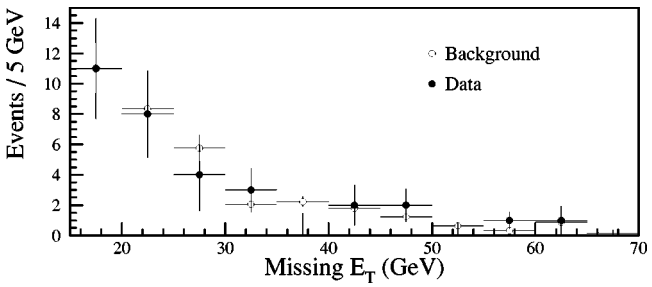

FIG. 1. Comparison of the $\not\!\!E_T$ distributions for data and background for $ee+1$-jet events (see text).

Our data sample was further refined by requiring two good jets with $E_T>20$ GeV, $\not\!\!E_T>20$ GeV, a fiducial cut on the event vertex [3], and offline lepton selections of $E_T(e_1)>17$ GeV and $E_T(e_2)>15$ GeV, or $E_T(e)>17$ GeV and $E_T(\mu)>4$ GeV, or $E_T(\mu_1)>20$ GeV and $E_T(\mu_2)>10$ GeV. This left 10 ee, 6 $e\mu$, and 3 $\mu\mu$ events.

Background came from four sources: $t\bar{t}$, Z and W boson, and QCD jet production. The $t\bar{t}$ and Z boson backgrounds were calculated using published cross sections [10,11] and a fast detector-simulation package (described below), while QCD multijet and $W+$jets backgrounds were estimated from data. For the ee and $e\mu$ signatures, we selected events with nearly the same topology, except that one isolated electron was missing and an extra jet was required in its place. The background was then estimated using the measured probability of one of the jets being misidentified as an isolated electron [3]. For $\mu\mu$ signatures, the background sample was defined by one isolated and one non-isolated muon (within a jet), and two or three other jets. The measured probability for a non-isolated muon to appear as an isolated muon was used to estimate the background from this source [9]. The QCD and $W+$jets backgrounds were combined because they are topologically similar: for W boson events, the identified lepton is real, and for QCD the identified lepton is due to a jet fluctuation. For the accepted ee and $\mu\mu$ events, about 50% of the background results from Z boson production, 30% from QCD/$W+$jets, and 20% from $t\bar{t}$ production. For the accepted $e\mu$ events, the breakdown was 10%, 60%, and 30%, respectively.

The uncertainties in the QCD/$W+$jets backgrounds stemmed from the energy scale (12%), the probability of lepton misidentification (15%), and statistics (2–100 %). The uncertainties in the other backgrounds were due to trigger and identification efficiencies (11–15 %), cross section (8–30 %), energy scale (2%), and Monte Carlo statistics (2–50 %). The large statistical uncertainties dominate only when backgrounds are negligible (<0.1 events).

To check for systematic uncertainties in misidentification of electrons, we enlarged our ee event sample by 32 events by selecting interactions that contained two good electrons and at least one jet. The $\not\!\!E_T$ for these 42 events is compared in Fig. 1 with the analogous background estimate from QCD/$W+$jets. The two distributions in Fig. 1 were normalized to each other in the 15–20 GeV interval, where background dominates, and are seen to be consistent over the entire range of $\not\!\!E_T$, thereby supporting an assertion that the selected ee events are consistent with mismeasurement (or fluctuation) of energy in the calorimeter.

The usual way to search for a signal is to generate signal and background events and then optimize a single set of requirements that yields the best discrimination. A problem with this method is that the optimum thresholds vary as a function of the mSUGRA input parameters. In essence, one must select different requirements at every point in model space, which demands exceptional computing resources.

In this Rapid Commuication, we describe a novel method for performing an approximate optimization of selection criteria on a grid of thresholds, as exemplified in Table I. For ee signatures, we considered sets of requirements both with and without an exclusion of ee invariant mass (M_{ee}) around the Z boson mass. For $\mu\mu$ signatures, a cut of $\not\!\!E_T>40$ GeV provided the best reduction in the Z boson background. Each unique combination of thresholds is called a channel. In all, we defined 16 ee, 24 $e\mu$, and 12 $\mu\mu$ channels, for a total of 52. Later, we will describe our method for selecting the optimized channel within each dilepton signature, based on the specific point in the $(m_0, m_{1/2}, \tan\beta)$ space.

To handle the large number of channels, a specialized Monte Carlo program was written [3] that incorporated SPYTHIA [12] as the event generator. This Monte Carlo program used a fast simulation of the detector, the trigger, and particle identification, using efficiencies and resolutions from data, and calculated the probability of observing events in each of the 52 channels. The primary outputs were the efficiencies $\epsilon_i = B\cdot\varepsilon_{\rm trig}\cdot\varepsilon_{\rm id}\cdot a_{\rm det}$ (products of the branching fraction, trigger efficiency, identification efficiency, and detector acceptance, respectively) for each channel i, and the theoretical production cross section. The fast Monte Carlo program reproduced efficiencies obtained in a more detailed simulation to 1–2 % accuracy.

Because looser requirements produced event samples that were supersets of tighter requirements, the channels within a given signature are correlated. To avoid bias, we chose a best channel for each signature (repeated for each mSUGRA model analyzed) based on the background estimate and expected signal [13]. Specifically, for each model k, where k denotes a specific choice of m_0, $m_{1/2}$ and $\tan\beta$, we defined an expected significance for channel i: $\overline{S_i^k} = \Sigma_{N=0}^{\infty} P(s_i^k + b_i|N)\cdot S(b_i|N)$, where P is the Poisson probability that signal, s_i^k, and background, b_i, produce N observed events, and S is the Gaussian significance, i.e. the number of standard deviations that background must fluctuate to produce N events [14]. Clearly, the sensitivity of the search, as reflected in the above sum over all N possible outcomes of the experiment, improves when the probabilities $P(s_i^k+b_i|N)$ are sizeable, but the likelihoods of b_i fluctuating to N are small [i.e., $S(b_i|N)$ are large]. The three maximum $\overline{S_i^k}$ values define three independent optimized search channels: $ee_{\rm best}^k$, $e\mu_{\rm best}^k$, and $\mu\mu_{\rm best}^k$. The single best of the two- or three-channel combinations ($cmb_{\rm best}^k$), is again defined by the analogous maximum $\overline{S_{cmb}^k}$, yielding four search channels per model.

For each model k, we calculated the four 95% confidence level (C.L.) limits on the cross section, $\sigma_{\rm lim}^x$ with $x=ee$, $e\mu$, $\mu\mu$, or cmb, using a standard Bayesian prescription, with a

TABLE I. Representative results for all signatures. For ee, $E_T(e_1)>17$ GeV and $E_T(e_2)>15$ GeV. For $\mu\mu$, the requirements were 10 and 20 GeV. For $e\mu$, each channel required $E_T(e)>17$ GeV, and $E_T(\mu)$ as specified, μ. For all signatures, the leading jet E_T is j_1, and we required $N_{\rm jets}$ with $E_T>20$ GeV. The uncertainty on the background is the sum in quadrature of systematic and statistical contributions. The probability is for the background to fluctuate to produce the number of observed events. $(\epsilon\sigma)_{\rm lim}$ is the 95% C.L. exclusion on the product of the total cross section, branching ratio, and all efficiencies, in fb.

j_1	$N_{\rm jets}$	$\not\!\!E_T$	Background	Data	Prob. (%)	$(\epsilon\sigma)_{\rm lim}$
Signature: $ee+{\rm jets}+\not\!\!E_T$						
20	2	20	10.67 ± 1.24	10	50.1	85
20	3	20	3.08±0.39	2	40.3	42
20	3	30	1.28±0.21	1	63.4	42
45	2	20	7.56±0.94	5	23.5	58
Signature: $ee+{\rm jets}+\not\!\!E_T$, excludes $80<M_{ee}<105$						
20	2	20	4.84±0.69	5	52.5	67
20	3	20	1.27±0.21	1	63.8	40
45	2	20	3.03±0.48	3	64.0	60
45	**3**	**20**	0.93±0.17	0	39.5	31
45	3	30	0.80±0.16	0	44.9	31
Signature: $\mu\mu+{\rm jets}+\not\!\!E_T$						
20	2	20	1.61±0.26	3	22.1	68
20	3	20	0.37±0.10	2	5.6	66
20	**2**	**30**	0.75±0.19	2	17.6	60
20	2	40	0.53±0.16	1	40.4	46
45	2	20	1.28±0.24	3	14.2	71
45	3	40	0.12±0.06	1	11.4	50
Signature: $e\mu+{\rm jets}+\not\!\!E_T$						
μ j_1	$N_{\rm jets}$	$\not\!\!E_T$	Background	Data	Prob. (%)	$(\epsilon\sigma)_{\rm lim}$
4 20	2	20	6.30±1.04	6	55.9	73
4 20	3	20	1.75±0.31	1	47.6	41
4 45	2	30	1.97±0.47	2	57.2	52
4 45	3	30	0.70±0.16	0	49.7	31
10 45	2	20	1.79±0.49	2	52.0	53
10 45	**3**	**20**	0.46±0.14	1	36.3	47
10 45	2	30	1.35±0.44	0	25.9	31
10 45	3	30	0.41±0.13	0	66.4	31

flat prior for the signal cross section [3]. We also calculated a model-independent limit for the product $\epsilon\cdot\sigma$. Table I summarizes the background predictions and the number of observed events in representative channels, and the (one-sided Poisson) probability that the background fluctuated to produce the observed events. Indicated in bold font are the three best channels for the model $\tan\beta=2$, $m_0=280$ GeV/c^2 and $m_{1/2}=51$ GeV/c^2 [these masses correspond to $m(\tilde{q})=306$ GeV/c^2 and $m(\tilde{g})=164$ GeV/c^2], where we obtained $\epsilon^{ee}=(0.049\pm0.005)\%$, $\epsilon^{e\mu}=(0.009\pm0.001)\%$, $\epsilon^{\mu\mu}=(0.024\pm0.002)\%$, and $\sigma^{ee}_{\rm lim}=58$ pb, for $\sigma_{\rm tot}=84$ pb.

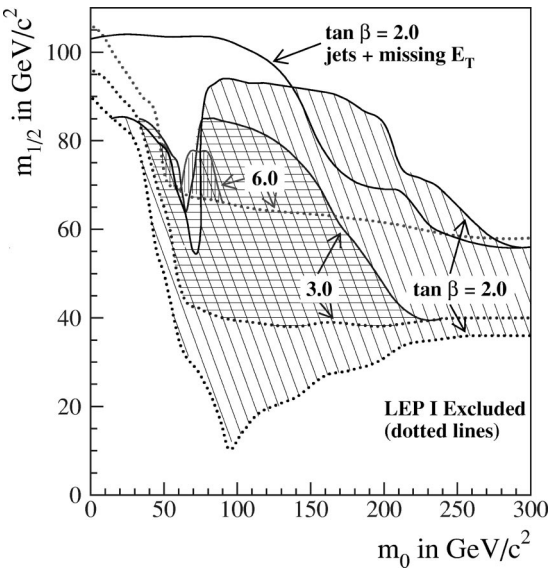

FIG. 2. The hatched regions are excluded by the dilepton search at the 95% C.L. for $\tan\beta=2$ (diagonal), 3 (horizontal), and 6 (vertical), with $A_0=0$ and $\mu<0$. The regions below the dotted lines are excluded by the CERN e^+e^- collider LEP I. The result from the DØ jets and $\not\!\!E_T$ search [4] is also shown.

We generated about 10 000 models, k, randomly in the $0<m_0<300$ GeV/c^2, $10<m_{1/2}<110$ GeV/c^2, and $1.2<\tan\beta<10$ space, to obtain a rough exclusion region. Near the boundary of the m_0 and $m_{1/2}$ exclusion region, higher statistics samples were generated for several values of $\tan\beta$. Figure 2 shows the 95% C.L. exclusion regions for $\tan\beta=2$, 3, and 6. Published results from the CERN e^+e^- collider LEP I [15] and DØ for the jets + $\not\!\!E_T$ channel [4] are shown for comparison. For $\tan\beta>6.0$, we do not exclude models not previously excluded by LEP I. (Recent results from LEP II [16] provide limits comparable to those presented in this Rapid Communication.)

The contours in Fig. 2 have a structure that can be understood as follows. First, the dip near $m_0=80$ GeV/c^2 for $\tan\beta=2.0$ is caused by the dominance of the decay $\tilde{\chi}^0_2\rightarrow\nu\bar{\nu}\tilde{\chi}^0_1$ over $\tilde{\chi}^0_2\rightarrow l^+l^-\tilde{\chi}^0_1$ in this region of phase space. Sensitivity improves for $\tan\beta$ closer to 3.0 due to several factors: gaugino mass couplings increase, causing the $\tilde{\chi}^0_2$ to preferentially decay into quarks and become a source of jets; gaugino masses decrease, and decays of squarks into $\tilde{\chi}^0_3$ and $\tilde{\chi}^0_4$ become allowed; $\tilde{\chi}^0_3$ and $\tilde{\chi}^0_4$ dominantly decay into sneutrinos, $\tilde{\nu}_l$; and $\tilde{\nu}_l\rightarrow\tilde{\chi}^\pm_1 l^\mp$ dominates in this region and becomes a source of leptons. Sensitivity decreases again for $\tan\beta$ values around 6.0, where decays into light charged leptons are reduced by increased couplings to large mass fermions. Second, the exclusion for $m_{1/2}$ decreases for large m_0, which corresponds to the region where $m_{\tilde{q}}\gg m_{\tilde{g}}$, and squark production does not contribute. In this asymptotic region, we exclude gluinos with masses below 175 GeV/c^2 for $\tan\beta=2.0$. For squarks and gluinos of equal mass, we exclude masses below 255 GeV/c^2 for $\tan\beta=2.0$. We also exclude gluinos below 129 GeV/c^2 and squarks below 138 GeV/c^2, for $m_0<300$ GeV/c^2 and $\tan\beta<10.0$.

In conclusion, we have performed a search for dilepton signatures from squark, gluino, and gaugino production. No significant excess of events was observed and we have presented our results in terms of contours of exclusion in mSUGRA parameter space.

We thank C. Kolda, S. Mrenna, G. Anderson, J. Wells, and G. L. Kane for helpful discussions. We thank the staffs at Fermilab and at collaborating institutions for contributions to this work, and acknowledge support from the Department of Energy and National Science Foundation (USA), Commissariat à L'Energie Atomique (France), Ministry for Science and Technology and Ministry for Atomic Energy (Russia), CAPES and CNPq (Brazil), Departments of Atomic Energy and Science and Education (India), Colciencias (Colombia), CONACyT (Mexico), Ministry of Education and KOSEF (Korea), CONICET and UBACyT (Argentina), A.P. Sloan Foundation, and the Humboldt Foundation.

[1] P. Nath *et al.*, *Applied N = 1 Supergravity*, ICTP Series in Theoretical Physics Vol. 1 (World Scientific, Singapore, 1984); H. Nilles, Phys. Rep. **110**, 1 (1984); H. Haber and G. L. Kane, *ibid.* **117**, 75 (1985); X. Tata, in *The Standard Model and Beyond*, edited by J. Kim (World Scientific, Singapore, 1991).

[2] For the models under consideration, $\tilde{\chi}_1^0$, the lightest neutralino is the LSP over most of the mSUGRA parameter space.

[3] R. J. Genik II, Ph.D. thesis, Michigan State University, http://www-d0.fnal.gov/results/publications_talks/thesis/thesis.html

[4] DØ Collaboration, B. Abbott *et al.*, Phys. Rev. Lett. **82**, 29 (1999).

[5] L. E. Ibañez, C. Lopez, and C. Muñoz, Nucl. Phys. **B256**, 218 (1985); M. Drees and M. M. Nojiri, *ibid.* **B369**, 54 (1992); H. Baer and X. Tata, Phys. Rev. D **47**, 2739 (1993).

[6] G. L. Kane, C. Kolda, L. Roszkowski, and J. Wells, Phys. Rev. D **49**, 6173 (1994).

[7] DØ Collaboration, S. Abachi *et al.*, Nucl. Instrum. Methods Phys. Res. A **338**, 185 (1994).

[8] DØ Collaboration, B. Abbott *et al.*, Nucl. Instrum. Methods Phys. Res. A **424**, 352 (1999).

[9] DØ Collaboration, B. Abbott *et al.*, Phys. Rev. D **58**, 052001 (1998).

[10] DØ Collaboration, B. Abbott *et al.*, Phys. Rev. D **60**, 012001 (1999).

[11] DØ Collaboration, B. Abbott *et al.*, Phys. Rev. D **60**, 052003 (1999).

[12] S. Mrenna, Comput. Phys. Commun. **101**, 232 (1997). SPYTHIA is a superset of PYTHIA 5.7 [13], allowing us to generate SM backgrounds. We incorporate routines developed by Kolda [6] to generate the mSUGRA model spectrum. This spectrum is passed to SPYTHIA using the general MSSM option.

[13] T. Sjöstrand, CERN-TH.7112/93.

[14] J. Linnemann, in *Proceedings of Computing in High Energy Physics*, Rio De Janiero, 1995 (World Scientific, Singapore, 1996).

[15] Particle Data Group, R. M. Barnett *et al.*, Phys. Rev. D **54**, 1 (1996), p. 165.

[16] ALEPH Collaboration, R. Barate *et al.*, Eur. Phys. J. C **11**, 193 (1999); OPAL Collaboration, G. Abbiendi *et al.*, *ibid.* **14**, 187 (2000); **16**, 707(E) (2000).